# High Transverse Momentum Physics at RHIC

*W.B.Christie*
*Brookhaven National Laboratory*
*Upton, New York*
*Presented at ICQGP, Jaipur India, March 1997.*

## Introduction

This paper is organized as follows. In section one some of the Physics motivations that make the high transverse momentum physics program at RHIC compelling are discussed. In section two some of the ways that one may use the information carried by the hard scattered partons to investigate some of the properties of the quark-gluon plasma which should be formed in heavy ion collisions at RHIC are described. In the third section one of the detectors being constructed at RHIC, the STAR detector, is described and some examples are given of how this detector is well suited to pursue the high transverse momentum physics topics at RHIC. Finally, section 4 contains a summary and some concluding remarks.

## 1. Physics Motivation

RHIC will be the first Heavy Ion accelerator in which a large fraction, on the order of 50%, of the energy transferred from the kinetic energy of the colliding beams to particle production comes from partonic processes that are calculable in perturbative Quantum Chromodynamics (pQCD). This ability to apply the well established tool of QCD to the heavy ion collisions at RHIC is vital to aid in the interpretation of the data that will be collected there.

At RHIC energies one may apply the pQCD down to Bjorken x ranges on the order of 0.02. If one has a pair of partons, each of which has a Bjorken x of 0.02, scattered into pseudorapidity 0, the mean momentum of the scattered partons will be ~ 2 GeV/c ( $X_{Bj} \approx {}^{2P_t}/_{\sqrt{s}}$). This is about as low in momentum as theorists feel confident in the application of perturbative QCD. At these small values of $x_{Bj}$ the gluons structure function is much larger than the quark structure function[1], as shown in Fig. 1. It is the scattering of these soft gluons that will account for about half of the energy transferred from the projectile frame into

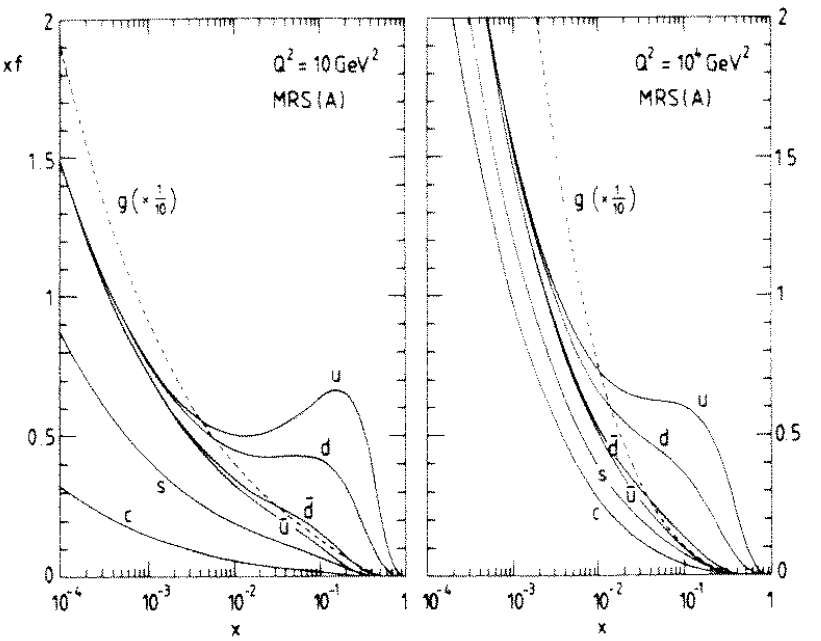


*Fig. 1. MRS(A) partons shown as a function of x at $Q^2$ = 10 and $10^4$ $GeV^2$.*

midrapidity at RHIC and drive the formation of the very high energy density volume which we'd like to study. The possible deconfined state resulting from this high density region will be referred to as a quark gluon plasma (QGP).

The dominance of the soft gluons in the development of the QGP is illustrated in what was become known as the "Hot Glue" scenario, originally developed by E. Shuryak[2], with further investigations by E. Shuryak and L. Xiong[3]. Shuryak argues that as the gluons dominate the nucleon structure functions for small values of Bjorken x, the initial scattering of the soft gluons associated with the colliding nuclei leads to a very hot, nonequilibrium system of gluons. Shuryak further argues that as the elastic scattering rate ($gg \rightarrow gg$) is two orders of magnitude larger than the lowest order gluon-quark transition process ($gg \rightarrow q\bar{q}$), that the gluons are the major component of the early stages of the plasma development. The large elastic scattering cross section for the gluons leads to a very rapid kinetic equilibration of the gluons, $\tau_{KE} \sim 0.3$ fm/c. Table 1 lists the temperature and time estimates for the gluons and quarks when they reach kinetic equilibrium.

Table 1

| | $T_g$(MeV) l | $\tau_g$(fm/c) l | $T_g$(MeV) l+s | $\tau_g$(fm/c) l+s | $T_q$(MeV) l+s | $\tau_q$(fm/c) l+s |
|---|---|---|---|---|---|---|
| RHIC | 340 | 1 | 500 | 0.3 | 200 | 2 |
| LHC | 440 | 0.8 | 660 | 0.25 | 260 | 1.7 |

*Table 1, from Shuryak[2]. Initial gluonic and quark temperatures and equilibration times, estimated with only large-angle scattering (l) or both small- and large-angle ones (l+s).*

This initial temperature of the gluons is about twice as high as some previous estimates. Shuryak points out that this should lead to increases in the production of charm and strange quarks, as well as modifications to the photon and dilepton spectra.

Starting with the kinetically equilibrated gluons, Xiong and Shuryak studied how this expanding system would evolve, including gluon multiplication ($gg \rightarrow ng$). In particular they investigated under what conditions the gluons would reach chemical equilibration, and how long the temperature of the system would remain above the critical temperature. They parameterized the gluon distribution function as:

$$f(p,\tau) = \xi(\tau)\exp[-p/T(\tau)]$$

$\xi(\tau)$ is defined as the "fugacity". Chemical equilibrium is reached when the chemical potential vanishes. In this parameterization this occurs when $\xi(\tau) \approx 1$. Some of the results from their paper are shown in Fig. 2.

As shown in Fig. 2, if the gluon system starts with a large initial fugacity, it quickly reaches chemical equilibrium. In the time period between the kinetic and chemical equilibrium the system cools very rapidly. This is due to the conversion of thermal energy into gluons in the gluon multiplication process. Once chemical equilibrium is reached one sees that the system cools more slowly, due to just the adiabatic expansion. The evolution plots shown in Fig. 2 stop when the temperature of the system reaches Tc (~170 MeV).

The general lesson that one gets from this study is that the lifetime of the plasma state depends critically on the initial conditions for the system. If one starts with a large initial fugacity the system rapidly reaches chemical equilibrium and then cools relatively slowly to the critical temperature, leading to a long lifetime in the plasma state. The converse is that if the initial fugacity is low the system cools rapidly for a longer period

before the adiabatic cooling sets in, leading to a short plasma lifetime. If the initial fugacity is too low the system may never reach chemical equilibration before it cools to $T_c$.

Other interesting features of the evolution of the parton plasma, including some plots of the quark fugacities, can be found in a report by X.N. Wang[4].

An important input to the determination of the initial conditions of the gluon distribution resulting from the heavy ion collisions at RHIC is the gluon structure function down to about 0.02 or so in Bjorken x. The gluon structure functions are not well known at present, even for single nucleons. There is an additional complication that one must deal with for nucleons bound in nuclei. This is the modification (depletion) of the quark structure function at small values of $x_{BJ}$ known as nuclear shadowing. While not yet measured, it is plausible to assume that this nuclear shadowing will also appear in the structure function for the gluons. These structure function measurements can be made at RHIC.

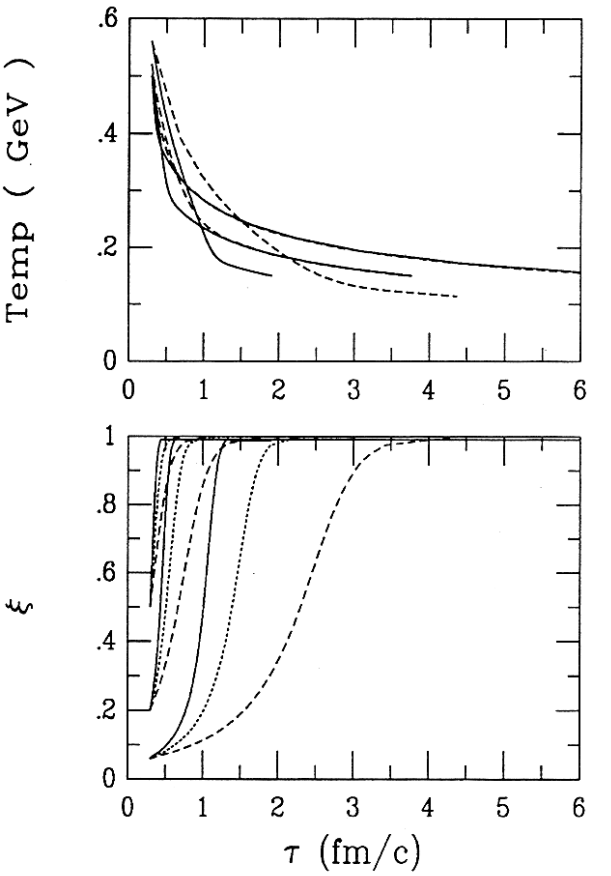


*Fig 2. The time evolution of the gluon fugacity($\xi$) and temperature in an expanding gluon plasma, for three sets of initial conditions ($T_i$(GeV),$\xi_i$)= (0.56,0.06), (o.5,0.25), and (0.5, 0.5). Please see ref. 2 for further details.*

## 2. Using the Energy loss of hard scattered partons to study the plasma

Granting that a quark-gluon plasma has been formed, there are a number of ideas on how one can attempt to study/measure its properties. One of these methods is to try to measure the energy loss of a parton traversing the plasma. There are two key reasons why this method is of interest. The first is that the processes that lead to the hard partons happen very early in the collision. As such they exist at the right period of time when the plasma may exist (~1→6 fm/c). The second reason is that the partons interact strongly with the plasma.

The energy loss for a parton can be thought of in terms of two processes[4]:

$dE_{el}/dx$ - that due to elastic simple scatterings

$dE_{rad}/dx$ - radiative energy loss due to induced radiation from multiple scatterings.

Studies[5] of $dE_{el}/dx$ at finite temperatures give a rather small logarithmic energy dependence (e.g. 0.2 - 0.5 GeV/fm for a quark Jet with E=30 GeV).

The dominant source of energy loss is thus expected to be via $dE_{rad}/dx$. There have been many estimates of $dE_{rad}/dx$ in the past. These estimates have varied widely.

How $dE_{rad}/dx$ behaves depends on the:

- Energy of the parton
- Color screening mass $\mu_D$ ($\mu_D^2 = 4\pi\alpha_s T^2\lambda_g$ Use $\lambda_g$=1 for equil. Plasma )
- Mean free path in the medium $\lambda_f$
- Effective formation time $\tau_{QCD}$ ($\tau_{QCD} = \frac{C_A}{2C_2}\frac{2\cosh y}{k_\perp}$)

There are a number of quantum interference effects that effect the radiative energy loss. One of these, the Landau-Pomeranchuk-Migdal (LPM) effect, plays a role in $dE_{rad}/dx$ by suppressing soft gluons whose formation time is longer than the mean free path between scatterings for the parton in the media.

There are two limits that one often encounters for the radiative energy loss of partons. The first is the "factorization" limit. In the factorization limit one fixes the product of the color screening mass and mean free path of the parton to be much greater than one, and lets the energy of the parton go to infinity (Fix $\mu_D \lambda_f >> 1$, let $E \rightarrow \infty$). This leads to a logarithmic energy dependence for the radiative energy loss.

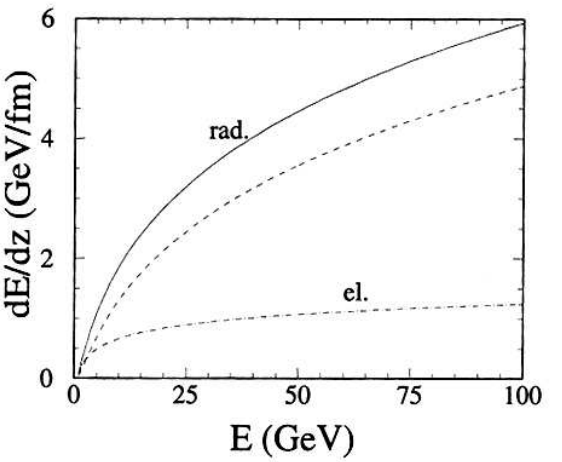


*Fig. 3. The energy dependence of the energy loss of a quark with energy E inside a quark-gluon plasma at temperature T=300 MeV. A weak coupling $\alpha_s$=0.3 is used. The solid line is the full expression and the dashed line is the factorization limit of the radiative energy loss. The dot-dashed line is the elastic energy loss.*

The second limit is known as the "Bethe-Heitler" limit. Here one fixes the energy of the parton, and lets the product of the screening mass and the mean free path go to infinity (Fix E, let $\mu_D \lambda_f \rightarrow \infty$). This leads to the situation where the mean free path is larger than the effective formation time, and the radiation from each of the scatterings add up. This leads to a linear dependence of the radiative energy loss on the energy. Fig. 3. shows the energy loss of a quark in a plasma as a function of the parton energy[4].

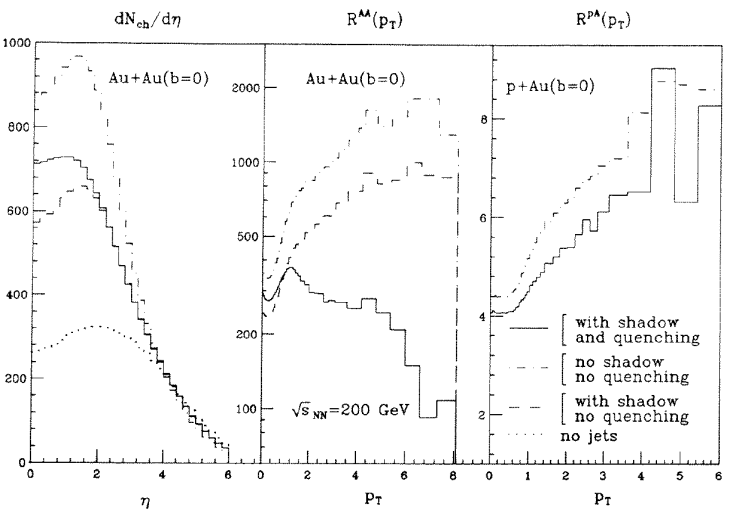


*Fig. 4. Results of HIJING on the dependence of the inclusive charged-hadron spectra in central Au+Au and p+Au collisions on minijet production (dash-dotted), gluon shadowing (dashed), and jet quenching (solid line) assuming that gluon shadowing is identical to that of quarks and dE/dl = 2 GeV/fm. $R^{AB}(p_T)$ is the ratio of the inclusive $p_T$ spectrum of charged hadrons in A+B collisions to that in p+p.*

A recent study[6] of $dE_{rad}/dx$ by Dokshitzer, Baier, Peigne and Schiff showed that dE/dx may grow linearly with the length of medium traversed, L.

The idea of using the energy loss of a parton in the plasma to look for a signature of the existence of the plasma in ultra relativistic heavy ion collisions gained wide attention with a publication[7] by X.N.Wang and M.Gyulassy. They demonstrated with the HIJING event generator model that one may be able to look for effects of gluon shadowing and energy loss in dense partonic matter via inclusive, moderate Pt (≤ ~8 GeV/c), single particle spectra. This idea is illustrated in Fig. 4, which is from their paper.

A point that should be kept in mind when contemplating the measurement and interpretation of the single particle $P_t$ spectrum is that to extract the amount of parton energy loss (i.e. quenching), if any, one must know how large the effect, if any, is due to the nuclear shadowing. The contribution due to the nuclear shadowing can be determined by measuring the gluon structure functions in the proton, and for nucleons bound in a gold nucleus.

In a subsequent study by Wang, Huang, and Sarcevic[8], a technique is proposed where one tries to extract the parton energy loss in the medium using events that have a tagged direct photon. The physics that one is after, the energy loss of the parton in the dense medium, is the same as in the paper by Wang and Gyulassy. The idea is that one looks in the opposite transverse direction of the tagged photon, and measures the $P_t$ spectrum of the charged particles. Modulo initial state interactions one then assumes that the Jet $E_t$ in this region is equal to that of the photon. One then looks at the modification of the fragmentation function for the jets, as a function of the jet (tagged photon) energy. The added advantage of using the photon tagged events is that knowing the Et of the hard scattered parton, it allows one to study

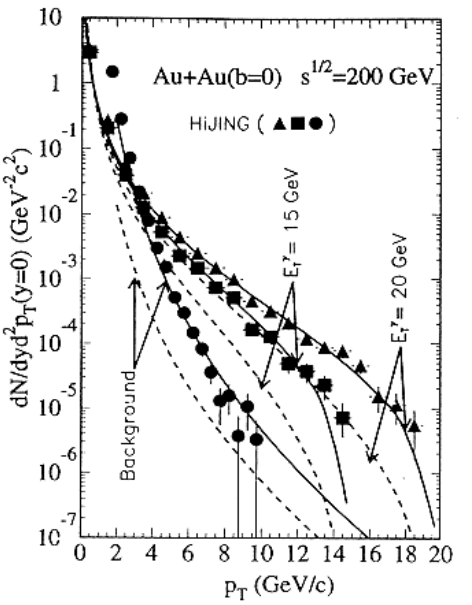


*Fig. 5. The differential Pt spectrum of charged particles from the fragmentation of a photon-tagged jet with $E_t^\gamma$=15 and 20 GeV and the underlying background in central Au + Au collisions at $\sqrt{s}$=200 GeV. The direct photon is restricted to $|y| \leq \Delta y/2 = 0.5$. Charged particles are limited to the same rapidity range in the opposite direction of the photon (±0.5 units in φ). Solid lines are perturbative calculations and points are HIJING simulations of 10k events. The dashed lines are calcs. with jet energy loss $dE_q/dx$ = 1 GeV/fm, and mean free path $\lambda q$ = 1 fm.*

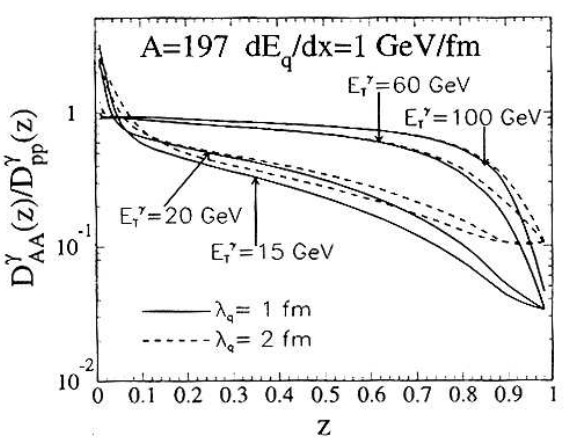


*Fig. 6. Ratio of the inclusive fragmentation function of a photon-tagged jet with and without energy loss in central Au+Au collisions for a fixed dEq/dx = 1 GeV/fm.*

the modification of the fragmentation function as a function of both z and the initial parton Et. Figs. 5, 6, and 7 are from their paper. In Fig. 5 ones sees that for a fixed dEq/dx and a fixed mean free path for the quark in the media, one expects a "softening" of the away side inclusive $P_t$ spectra.

Fig. 6 shows the ratio of the jet fragmentation functions for photon tagged events in AA collisions divided by that for pp collisions. By looking at the high z end of the fragmentation function ($z = P_t/E_T^{jet}$) one can get some information on the mean free path of the parton (i.e the probability that the parton suffers an inelastic collision in the media). This same ratio of fragmentation functions is shown in Fig. 7, as a function of the mean energy loss for the parton in the media, at a fixed, intermediate value of z. The point here is that by measuring the relative suppression of the fragmentation function in the intermediate z region one can extract information on the mean energy loss for the jet in the media.

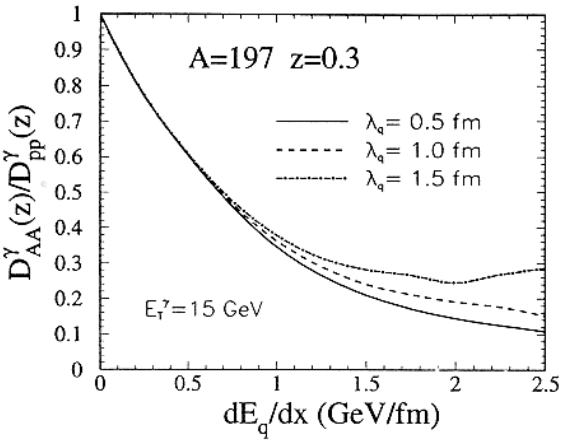


*Fig. 7. Ratio of the inclusive fragmentation function of a photon-tagged jet with and without energy loss in central Au+Au collisions at z = 0.3 as a function of dEq/dx.*

This same technique, using events with a tagged photon, was revisited in a subsequent paper by Wang and Huang[9]. In this paper they looked in more detail at what the effects of the initial and final state interactions would do to this analysis. A dramatic effect that is shown in the paper is that due to what they term $E_T$-smearing of the initial $E_T$ of the hard scattered parton in the tagged photon jet events. Using the HIJING Monte Carlo event generator, they selected events with some fixed direct photon energy around midrapidity (e.g. 10 GeV), and then looked at the $E_T$ of the away side scattered hard parton. What one sees is that the away side parton has a fairly wide distribution of transverse energies, due to the initial state interactions of the incoming partons. The average $E_T$ values for these away side partons is less than the $E_T$ of the photons. The explanation for this result is that as the cross section for producing a direct photon drops very rapidly as a function of $E_T$, when one "triggers" or selects an event with a given value of $E_T$ it is most likely that there was an initial Pt value for the two interacting partons in the direction of the detected photon. Fig. 8 shows

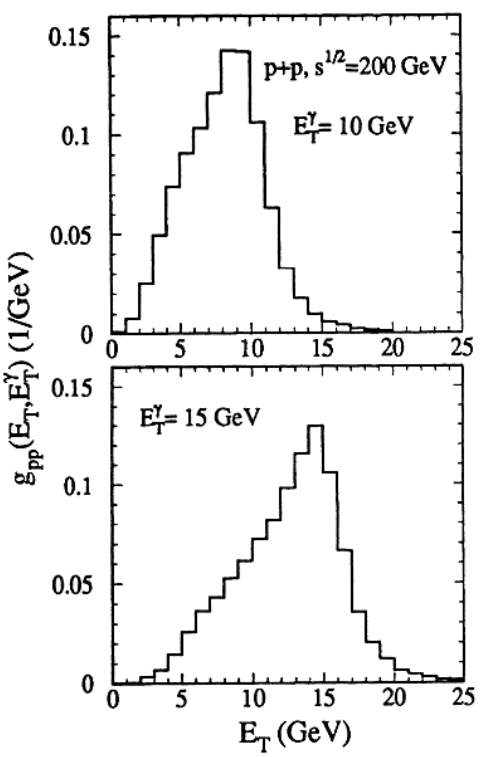


*Fig. 8 The $E_T$-smearing function for the photon-tagged parton jets with $E_T^\gamma$ = 10, 15 GeV, from HIJING simulations of pp collisions at $\sqrt{S}$ = 200 GeV. The averaged value of $E_T$ is $\langle E_T \rangle$ = 8.08, 12.57 GeV, respectively.*

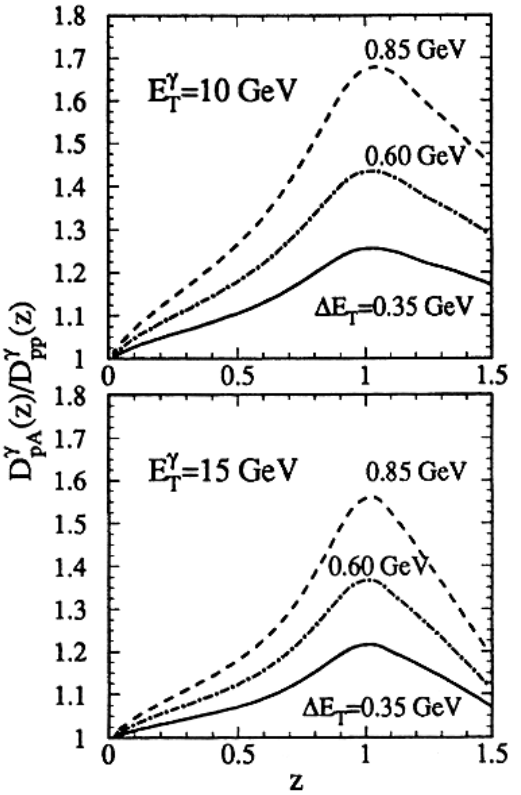


*Fig. 9. The modification factor for the photon-tagged jet fragmentation function in pA collisions with $E_T^\gamma$ = 10 and 15 GeV at $\sqrt{S}$ = 200 GeV, for different values of $\Delta E_T$ due to $E_T$ broadening.*

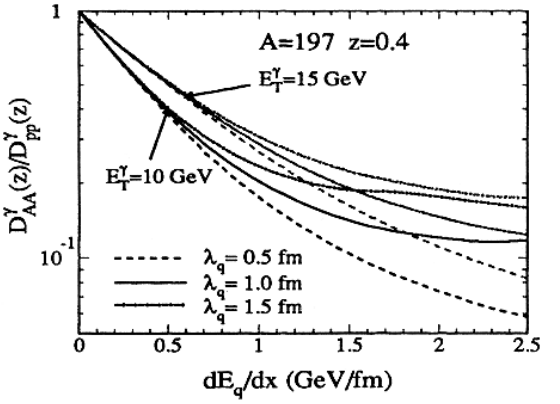


*Fig. 10. The modification factors for the inclusive fragmentation function of photon-tagged jets at given $z = p_T / E_T^\gamma$ = 0.4 as functions of parton energy loss dEq/dx with different values of the mean-free-path $\lambda q$, in central Au + Au collisions at $\sqrt{S}$ = 200 GeV.*

these away side $E_T$ distributions for pp events with 10 and 15 GeV $E_T$ photons.

Wang and Huang go on in this paper to offer a way to measure and take into account this $E_T$ smearing. The technique is that one looks at the ratio of the fragmentation functions in pA and pp collisions for events with a given $E_T$ direct photon. One can then parameterize the width of the bump in this ratio around $z \approx 1$, and then use this parametrization to account for the $E_T$ smearing in AA collisions. Fig. 9, from their paper, shows what this ratio of the fragmentation functions would look like for various widths of this smearing function.

Fig. 10, also from the same paper, shows how the information about the mean free path of the fast parton, as well as the average energy loss for the parton, in the dense medium/plasma, can be extracted from the modification of the jet fragmentation functions.

## 3. The STAR Detector at RHIC

The STAR detector, presently in the construction/assembly stage, is well suited to making the necessary measurements to study the physics topics discussed in the first two sections of this paper.

The STAR detector is a large acceptance device capable of tracking the large multiplicity of charged particles expected to be observed at RHIC. The baseline detector is a cylindrical Time Projection Chamber (TPC) located inside of a solenoidal magnet with a 0.5 T field to provide tracking, momentum analysis and particle identification of most of the charged particles at midrapidity. Momentum measurements will be made over a large pseudo-rapidity range ($|\eta| < 2$) with full azimuthal coverage ($\Delta\phi = 2\pi$). The Central Trigger Barrel (CTB), consisting of 240 scintillator slats, lies just outside of the TPC outer

field cage and gives charged particle multiplicity information for $|\eta| \leq 1$ and $2\pi$ in azimuth. Vertex Position Detectors (VPD), consisting of lead converter directly in front of phototubes, are placed around the beam pipe on each side of the interaction region. The CTB ($|\eta| \leq 1$), VPD ($4.8 \leq |\eta| \leq 5.0$), and direct readout of the wire planes incorporated in the TPC readout sectors ($1 \leq |\eta| \leq 2$) will be utilized to supply trigger information to STAR and luminosity information to both the STAR detector and the RHIC accelerator.

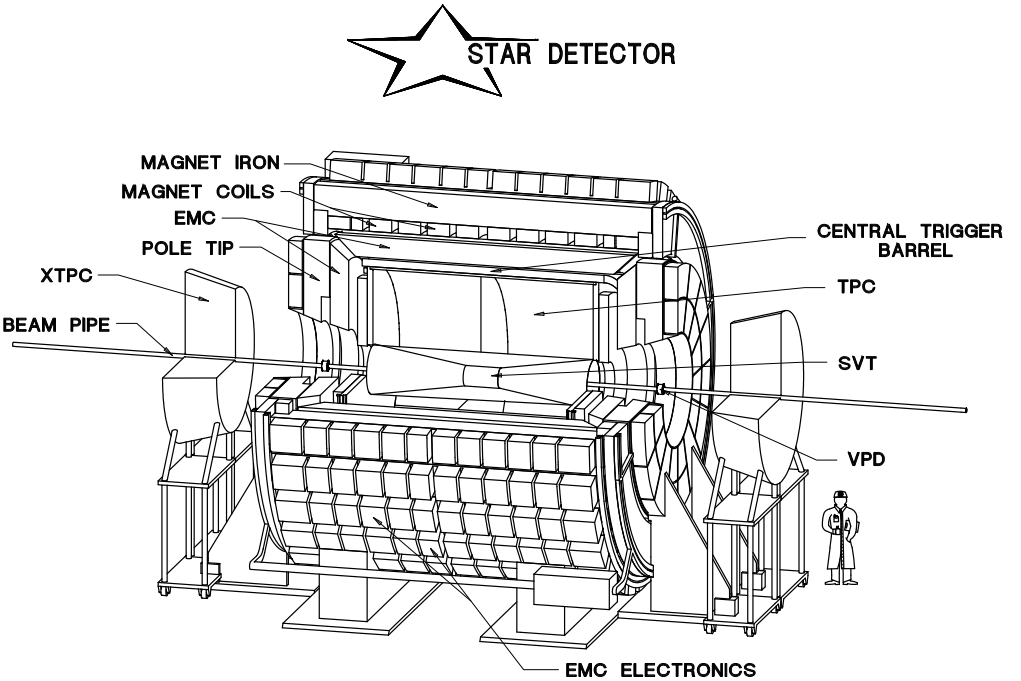


*Fig. 11. Cutaway view of the STAR detector. The XTPC which is shown in the figure as being outside of the STAR magnet has been redesigned. It is now inside of the solenoid and referred to as the FTPC.*

Improvements planned and proposed for STAR should significantly increase its physics capabilities. These additional detectors are the Silicon Vertex Tracker (SVT), an Electro-Magnetic Calorimeter (EMC), a highly segmented Time-of-Flight array (TOF), Forward Time Projection Chambers (FTPC), and a Photon Multiplicity Detector (PMD). The addition of the EMC is imperative for the physics study presented here. A cutaway view of the STAR detector is shown in Fig. 11.

As input to the calculation of the initial conditions for collisions at RHIC one wants to measure the gluon structure functions in the proton, as well as for nucleons bound in a nucleus. The most straight forward technique to measure these structure functions is through what is often referred to as QCD Compton scattering, where a quark and gluon scatter leading to a final state with a direct

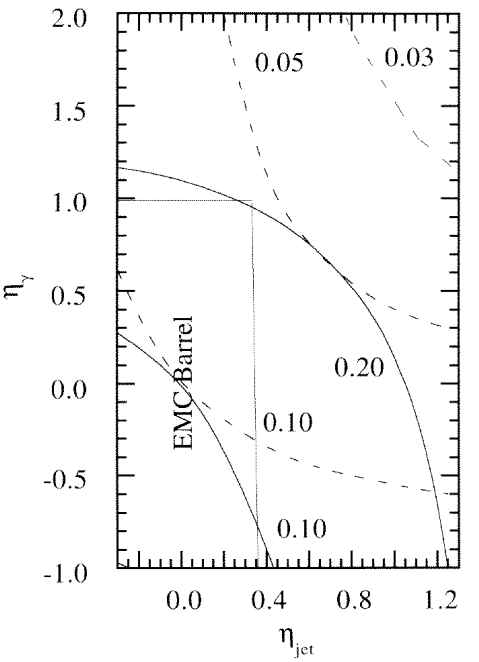


*Fig. 12. Acceptance of STAR EMC (barrel + 1 endcap). Please see text for interpretation.*

photon and a Jet (i.e. qg → γJet). By measuring the energy of the photon and the Jet as well as their pseudorapidities, one can calculate the values of $x_{BJ}$ for the scattered quark and gluon.

An important consideration when evaluating the ability of the STAR detector to make the measurement of the gluon structure function is the range of Bjorken x over which one can make the measurement. This acceptance is determined by how low in $E_T$ one can reconstruct the jet and the photon, and the geometrical acceptance of the detector. These quantities are shown in Fig. 12. The vertical axis is the pseudorapidity of the γ and the horizontal axis is that of the jet for a qg → γ-jet event. The rectangular box in the lower left hand corner shows the acceptance for the barrel EMC alone. One sees that if $|\eta_\gamma|$ is ≤ 1.0 and $|\eta_{jet}|$ ≤ ~0.35 then the event is within the acceptance of the barrel. The η range for the jet in the barrel is due to the finite (~0.7) radius typically used in jet finding codes and the requirement that all of the jet energy is intercepted by the barrel. The large increase in acceptance that one achieves with the addition of a single endcap EMC is shown by the area of Fig. 13 which is outside of the rectangular (EMC barrel) box. The range of Bjorken x is shown in Fig. 13 with the dashed (gluon x value) and solid (quark x value) curved lines. The curve is not shown in this plot, but the lowest x value accessible for the gluon, ~0.02, has some acceptance in the upper right hand corner. The Bjorken x values shown in Fig. 13 are for events with photons and Jets with $E_T$ = 10 GeV.

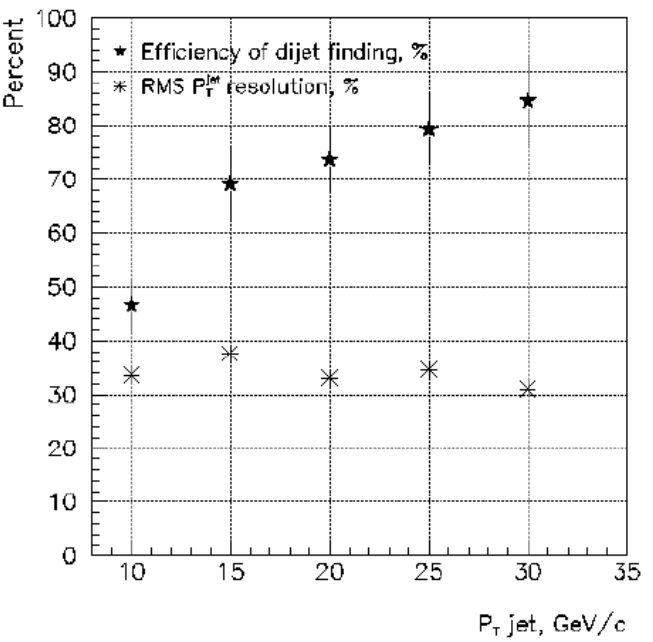


*Fig. 14. Jet efficiencies and resolutions versus Pt for $\sqrt{s}$ = 200 GeV pp events.*

Shown in Fig. 14 are some of the results of a simulation and analysis study[10] of the Jet finding efficiency and energy resolution for the STAR detector, including the electromagnetic calorimeter. The results shown are for pp events at $\sqrt{s}$ = 200 GeV. The efficiency values in the figure are for reconstructing both of the Jets in a di-jet event. For more details on this jet finding study please consult reference 10.

The next question to be addressed is whether or not one can gather enough of the right type of events to persue the analyses discussed earlier in this paper. In tables 2, 3, and 4 the cross sections and event rates are shown for Jets and direct photons. The cross sections were taken from a compilation put together by the Hard Probes collaboration[11]. The luminosities used in the calculation are shown in the table headings. A rather curious result is that the photon and Jet event rates are the same in the pp and pAu running. It comes out this way because the luminosity drops by a factor of 200 going from pp to pAu, whereas the cross section for hard processes goes up by about a factor of 197 (A of Au). The cross sections and rates are given per unit of pseudorapidity (η). The reader is

reminded that with the barrel EMC and one endcap STAR's coverage for photons will cover about 3 units in η. For well contained jets the coverage is about 1.5 units of η.

From the event rates it appears that it will take moderately long data runs, on the order of 100 days each, to get the γ-jet and di-jet statistics necessary for the measurement of the gluon structure functions. Recall that it is the low Pt jet and γ-jet events that yield information on the structure functions in the most important range of $x_{BJ}$ (down around 0.02).

Table 2. pp, $\sqrt{s}$ = 200 GeV, $L = 1 \times 10^{31}$ cm$^{-2}$s$^{-1}$, Rate = $\sigma \cdot L$

| $P_t$ (GeV/c) | $\sigma_{jet}$ $d^2\sigma/dp_t dy$ (μb/GeV) | Jet Rate (Hz/η·GeV) | $\sigma_\gamma$ $d^2\sigma/dp_t dy$ (ηb/GeV) | γ Rate (Hz/η·GeV) | γ Rate (#/100 days·η·GeV) |
|---|---|---|---|---|---|
| 5 | 122.7 | 1227 | 14.7 | 0.147 | $1.27 \times 10^6$ |
| 10 | 3.0 | 30 | 0.54 | $5.4 \times 10^{-3}$ | $4.67 \times 10^4$ |
| 15 | 0.26 | 2.6 | 0.06 | $6.0 \times 10^{-4}$ | 5184 |
| 20 | 0.037 | 0.37 | 0.01 | $1.0 \times 10^{-4}$ | 864 |
| 25 | 0.006 | 0.06 | 0.002 | $2.0 \times 10^{-5}$ | 173 |

Table 3. pAu $\sqrt{s}$ = 200 GeV, $L = 5 \times 10^{28}$ cm$^{-2}$s$^{-1}$, $\sigma_{pAu} = 197 \cdot \sigma_{pp}$

| $P_t$ (GeV/c) | $\sigma_{jet}$ $d^2\sigma/dp_t dy$ (μb/GeV) | Jet Rate (Hz/η·GeV) | $\sigma_\gamma$ $d^2\sigma/dp_t dy$ (ηb/GeV) | γ Rate (Hz/η·GeV) | γ Rate (#/100 days·η·GeV) |
|---|---|---|---|---|---|
| 5 | $2.42 \times 10^4$ | 1210 | 2896 | 0.145 | $1.25 \times 10^6$ |
| 10 | 591 | 29 | 106 | $5.3 \times 10^{-3}$ | 45790 |
| 15 | 51 | 2.6 | 11.8 | $5.9 \times 10^{-4}$ | 5098 |
| 20 | 7.3 | 0.36 | 2.0 | $1.0 \times 10^{-4}$ | 864 |
| 25 | 1.2 | 0.06 | 0.4 | $2.0 \times 10^{-5}$ | 173 |

Table 4 AuAu, $\sqrt{s}$ = 200 GeV, $L = 2 \times 10^{26}$ cm$^{-2}$s$^{-1}$ $\sigma_{AuAu} = 3880 \cdot \sigma_{pp}$ (10% central trig.[11])

| $P_t$ (GeV/c) | $\sigma_{jet}$ $d^2\sigma/dp_t dy$ (μb/GeV) | Jet Rate (Hz/η·GeV) | $\sigma_\gamma$ $d^2\sigma/dp_t dy$ (ηb/GeV) | γ Rate (Hz/η·GeV) | γ Rate (#/100 days·η·GeV) |
|---|---|---|---|---|---|
| 5 | $4.76 \times 10^5$ | 95 | $5.7 \times 10^4$ | 0.011 | 95040 |
| 10 | $1.16 \times 10^4$ | 2.3 | 2095 | $4.2 \times 10^{-4}$ | 3629 |
| 15 | 3026 | .6 | 233 | $4.7 \times 10^{-5}$ | 406 |
| 20 | 431 | $8.62 \times 10^{-2}$ | 39 | $7.8 \times 10^{-6}$ | 67 |
| 25 | 70 | $1.4 \times 10^{-2}$ | 7.8 | $1.6 \times 10^{-6}$ | 14 |

From looking at the rates in table 4 it appears that it will take a fairly substantial integrated luminosity to extract the structure functions in AuAu for photon-tagged events to study their modification by the media. For this study one would ideally like to have a good sample of events at $E_T$ values in the 10 to 15 GeV range or higher. As the value of $E_T$ increases the effect by the initial state interactions (i.e. the $E_T$ broadening) become less

prominent. Wang and Huang[9] argue in their paper that for AuAu collisions at RHIC the minimum value of $E_T^{\gamma}$ for the photon tagging of events is about 6 GeV. For $E_T^{\gamma}$ values above this minimum value their simulations indicate that the moderate to high $P_t$ tracks on the away side from the photon will be above the background. It appears that to gather sufficient statistics at the baseline AuAu luminosity that one will have to run for on the order of 300 days or so. If one is only interested in studying the single particle inclusive spectra, one can gather sufficient statistics much more quickly.

The final question which one must address is the efficiency to trigger on the events of interest for these studies, while at the same time looking to see whether STAR can handle these trigger rates. A very good simulation study of this question has been performed by Hubner, Westfall, and VanderMolen[12]. For this study a large number of pp and pAu events were generated using the HIJING event generator code. Events were created with no hard scattered partons (no jet events), with di-jets of various fixed $P_t$s, and with γ-jets of various fixed $P_t$s. These events were then passed through the STAR implimentation of the detector simulation code GEANT, with all of the material and geometry of the STAR detector in place, and with all the GEANT physics processes active. They then studied the trigger efficiencies and trigger rates for various sizes of patches of information from the electromagnetic calorimeter (i.e. 0.2 x 0.2, 0.4 x 0.4, etc., in η and ϕ) and for various energy thresholds placed on these EMC patches. In Fig. 15 one of the many plots from their study is shown. The rates shown in Fig. 15 are normalized with the cross sections for the various types and energies of events. By picking a threshold value for the maximum equivalent electromagnetic energy (sampled energy in the towers is taken by GEANT and scaled as though it is from purely electromagnetic energy incident on the calorimeter) in any of the 0.2 x 0.2 EMC patches, one can read off what the efficiency will be for a particular type of event, and what the total level 0 trigger rate will be. For example, if one sets the threshold at 7.5 GeV one would get a trigger rate of about 30 Hz. Depending on the rejection power of the level 1 and level 2 triggers for STAR, STAR can run with level 0 trigger rates from 100 to up several hundreds of Hz without suffering an unacceptably large (say greater than 50%) deadtime.

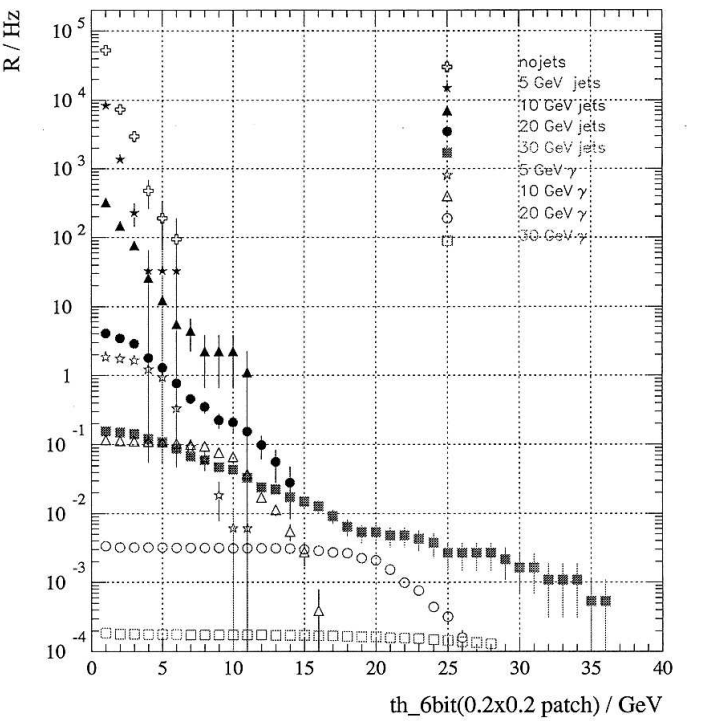


*Fig. 15. Rates at trigger level 0 versus the threshold at the maximum energy in a 0.2 x 0.2 patch for nojets (crosses), jets (filled symbols), and direct photons (open symbols) in pAu reactions for various energies as indicated in the picture.*

From this study one concludes that the triggering efficiency and raw level 0 trigger rate should not pose a problem for STAR in the pp and pAu running necessary for the physics analyses discussed in this paper. The trigger rates and efficiencies for the AuAu running, so that one can efficiently collect all of the events with an ~8 GeV or higher direct photon, while at the same time not being swamped with the rate from $\pi^0$ decays, requires further study. However, with the fairly low central collision rate (~100 Hz) for AuAu running with the baseline luminosity one does not have to be very selective to achieve an acceptable deadtime with a very high efficiency.

## 4. Summary and Conclusion

The development and evolution of the dense partonic matter formed in ultra relativistic heavy ion collisions is critically dependent on the initial conditions of the system. The fundamental input to calculations of these initial conditions is the gluon structure function. The event rates and acceptance of the STAR detector at RHIC will allow for the measurement of the gluon structure function in protons as well as in Nuclei.

The measurement of the energy loss of fast partons traversing the dense partonic matter appears feasible, as does the measurement of the modification of the fragmentation function for these partons. These measurements may well provide information on such properties as the density, lifetime, mean free path, and mean energy loss rate for the dense partonic matter or quark gluon plasma formed in these collisions.

---

[1] A.Martin, W.Stirling, R.Roberts, Phys.Rev.D**50** (1994) 6734.
[2] E.Shuryak, Phys.Rev.Lett. **68** (1992) 3270.
[3] L.Xiong and E. Shuryak, Phys.Rev.C, **49** (1994) 2203
[4] X.N.Wang, LBL-38145 (1996).
[5] J.D.Bjorken, Fermilab-Pub-82/59-THY (1982), M.Thoma, M.Gyulassy, Nucl.Phys.B351,491 (1991).
[6] Baier, Dokshitzer, Peigne, and Schiff, Phys.Lett. B345, 277 (1995), Baier, Dokshitzer, Mueller, Peigne, and Schiff, Nucl.Phys. B478, 577 (1996).
[7] X.-N.Wang and M.Gyulassy, Phys.Rev.Lett. **68**, 1480 (1992).
[8] X.N.Wang, Z.Huang, and I.Sarcevic, Phys.Rev.Lett. 77 (1996) 231.
[9] X.N.Wang and Z.Huang, LBNL-39742 (1996).
[10] W.Christie and K.Shestermanov, STAR Note #196. Available via STAR home page on the WWW.
[11] Hard Processes, Int.J.Mod.Phys. A10, 2881-3090, LBL-36948.
[12] B.Hubner, G.Westfall, and A.VanderMolen, STAR Note #276. Available via the STAR Home page on the WWW.